Electrocardiogram Baseline Wander Removal based on Empirical Mode Decomposition

Mohammadreza Ravanfar, Leila Azinfar, Riadh Arefin, Reza Fazel-Rezai

University of North Dakota, Grand Forks, USA

Abstract

In electrocardiogram (ECG) signals, low frequency artifacts caused by respiration and movements of patient and recording hardware, create challenging problems for signal processing algorithms. Due to nonlinear origins of these undesirable artifacts, the use of nonlinear signal processing methods gives assistance to achieve more reliable outcomes. This paper introduces a baseline drift cancellation algorithm using polynomial fitting based on empirical mode decomposition (EMD), then evaluates it comparing two conventional methods, EMD-based global slope minimization and moving average filtering. The methods were applied over 26 generated ECG baselines where the polynomial fitting showed more than 81% correlation with the generated baselines. The comparative results proved a remarkable robustness of the proposed algorithm against the baseline drifts.

1. Introduction

High qualified ECG signal has a key role in noninvasive diagnosis of heart abnormalities. However, there are different sources contaminating ECG signals. ECG intrinsic artifacts are caused by skin impedance, electromyography (EMG) noise, and electromagnetic interfaces [1]. The low frequency artifacts varying ECG offset are termed baseline wanders which can be caused by respiration and movements of patient and the recording hardware.

Due to uncertainties pertained to the baseline generation resources, the ECG baseline drifts show a non-stationary manner which negatively influences ordinary ECG processing algorithms. Thus, baseline correction still has remained as a challenging problem especially when unexpected movements of the patient or subject happen. The ECG signals have nonlinear characteristics as well which are typically understood by sharp changes, transitory drifts, and trends [2,3]. Therefore, nonlinear methods have more compatibility with ECG signal processing.

Due to the importance of ECG signal in health monitoring, there are high demands for improving ECG artifact removing methods. Thus, several approaches have been developed for baseline correction, of all of which moving average is the most popular baseline wander removal algorithm with high speed [4]. There are also algorithms emphasized on eliminating low frequency content of signal using finite impulse response (FIR) filters [5], adaptive filters [6], selective filters [7], and nonlinear filter banks [8]. Considerable number of papers attempted to extract baseline drifts through time-frequency domain and wavelet packets [9, 10]. In addition, some of popular pattern recognition approaches such as ICA and PCA have been applied for baseline wander removal [11,12].

Above all, in two recent decades, empirical mode decomposition (EMD) has found broad applications in ECG signal processing [13]. For instance, a systematic procedure including EMD-based high-pass filtering [14], multiband filtering approach [2], and global slope minimization [2] were introduced based on removing last intrinsic mode functions (IMFs)

2. Material and methods

2.1. Empirical mode decomposition

In 1998, Huang presented EMD method which is a suitable approach for processing non-stationary and nonlinear processes [14]. EMD is one of a few straightforward decomposition methods dealing with data directly and adaptively. The basic idea in EMD is that every signal is combination of IMFs including diverse oscillations. The main specification of modes is that they all have same number of extreme points and zero-crossings. Moreover, they have symmetry through their local means.

Summing IMFs results in original signal. Although IMFs have their own oscillatory modes, comparing to harmonic components in Fourier transform, IMFs have diverse amplitudes and frequencies in time domain. A given signal $x(t)$ can be decomposed as:

$$x(t) = h_1(t) + r_1(\mathrm{t}) \quad (1)$$

where $h_1(t)$ denotes first IMF and $r_1(t)$ shows residual signal. $h_1(t)$ should have two mentioned specifications. A given signal $x(t)$, can be written as:

$$x(t) = h^{(1)}(t) + r^{(1)}(\mathrm{t}) \quad (2)$$

where $h^{(1)}(t)$ denotes the first IMF and $r^{(1)}(t)$ shows the residual signal. The first IMF $h^{(1)}(t)$ should meet the two above conditions. For the next step the oscillatory mode of the residual signal $r^{(1)}(t)$ can be extracted, using the same process:

$$x(t) = h^{(1)}(t) + h^{(2)}(\mathrm{t}) + r^{(2)}(\mathrm{t}) \quad (3)$$

in which $r^{(1)}(\mathrm{t}) = h^{(2)}(\mathrm{t}) + r^{(2)}(\mathrm{t})$ and $h^{(2)}(\mathrm{t})$ is the second IMF of the signal $x(t)$. Therefore the original signal can be decomposed as:

$$x(t) = \sum_{k=1}^{K} h^{(k)}(t) + r^{(K)}(\mathrm{t}) \quad (4)$$

and also

$$x^{(k)}(t) = r^{(k-1)}(\mathrm{t}) \quad (5)$$

where k is the IMF number and K denotes the total number of IMFs. Huang's method can be summarized as following steps:

1) Find max points $u_n^{(k)}$ and min points $l_n^{(k)}$ of k^{th} IMF and n^{th} iteration and interpolate them to construct upper and lower envelopes $I_n^{u(k)}$ and $I_n^{l(k)}$.
2) Calculate mean envelope signal $m_n^{(k)}$ of $I_n^{u(k)}$ and $I_n^{l(k)}$ and then subtract it from $h_n^{(k)}$ to obtain $h_{n+1}^{(k)}$:
$$h_{n+1}^{(k)} = h_n^{(k)} - m_n^{(k)} \quad (6)$$
3) Repeat steps 1 and 2 until remove riding waves to obtain symmetrical waves (definitional conditions 1 and 2) [14] . This process is called sifting and the remained $h_n^{(k)}$ after n sifting is considered as i^{th} IMF.
4) Substitute $r^{(k)}(\mathrm{t})$ for $x^{(k)}(\mathrm{t})$ and repeat steps 1, 2 and 3 as far as stopping criteria is satisfied.

2.2. Global slope minimization (GSM)

As an EMD-based baseline removal method, global slope minimization was suggested in [2] where higher order IMFs are removed from the reconstructed signal and the global slope is computed in each step until stopping threshold is met. In this method, the signal is segmented into smaller parts. Then, two optional points are selected in each segment and the slope of the line drawn between them is determined. The lines' end points should be preferably positioned on P and T waves [2].

For a given ECG recording including T samples, M segments are considered for measuring the global slope where $x(t) = \sum_{m=1}^{M} x_m(t)$. The two points $(p_{m1}, p_{m2}) | \ m = 1, \dots, M$ are selected on each segment so that their within and between distances remain constant. The slopes of the lines $b_m^{(k')}$ are used to achieve the global slope by summation:

$$b_g^{(k')} = \sum_{m=1}^{M} \left| b_m^{(k')} \right| \quad (7)$$

in which k' denotes the number of last removed IMFs from reconstruction process. $b_g^{(k')}$ is calculated by removing each slow oscillatory mode. Then, the number of IMFs which should be removed from the reconstructed signal is specified when $b_g^{(k')}$ crosses the assigned threshold.

2.3. EMD-based polynomial fitting

we propose a modified polynomial curve fitting compatibilized with EMD, EMD-based polynomial fitting (EPF), in which there is no need to segment heart beats. Since in conventional polynomial fitting one point must be selected from each beat and using those representative points a polynomial curve is fitted to ECG signal [4].

Since ECG baseline intrinsically has slow fluctuations, an acceptable estimation of low frequency content of signal can be obtained from a low order polynomial equation. In other words, ECG baseline drifts can be modeled by fitting a polynomial curve to a recorded ECG, provided that the underlying ECG segment has a suitable length. The coefficients of the polynomial model can be easily reached by means of least square error (LSE). If the order of the equation is low, the mode is not able to provide a proper estimation of the baselines. On the other hand, if order of the model is higher than baseline's order, it partly tracks ECG basic wave instead of signal's trend. In EPF method, to consider a tradeoff between two, for a range of complexity, the model order is selected based on highest complexity (higher order). Indeed, the mean envelope of the estimated model is taken using cubic spline interpolation as follows:

$$m^{(k')} = (I_u{}^{(k')} + I_l{}^{(k')})/2 \quad (8)$$

where $I_u{}^{(k')}, I_l{}^{(k')}$ denote upper and lower envelopes, respectively, and k' is the number of last removed IMFs. After obtaining the mean envelope, to measure the contribution of each IMF in establishing the mean square error (MSE) of mean envelope is calculated:

$$MSE = \frac{1}{T} \sum_{t=1}^{T} \left| m^{(k')}(t) \right|^2 \quad (9)$$

Fig. 1 shows a typical ECG signal to which an artificial baseline has been added. The baseline is combination of a ramp and a truncated sin wave. The dashed line depicts mean envelope obtained from polynomial model. In EPF, the last IMFs are removed from reconstructed signal, and then MSE and the slope of the baseline are computed.

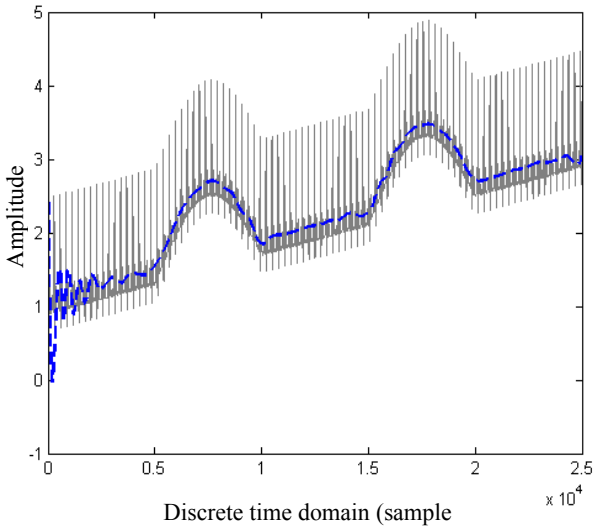

Figure 1. Baseline estimation of a typical ECG contaminated to an artificial baseline using EMD-based polynomial fitting.

When IMFs, being in charge of baseline drifts, are removed from signal reconstruction process, MSE logically decreases. Therefore, in removing last IMFs from reconstructed signal, the first IMF, whose MSE crosses the thresholds, stops the baseline correction algorithm.

3. Result and discussion

In order to evaluation of the EMD-based polynomial fitting, 26 artificial baselines were added to a typical ECG signal. Then the method was applied for ECG baseline correction process. In order to achieve a general insight into the performance of EPF method, it was compared with global slop minimization and moving average filtering.

There is no specific model for ECG baseline, therefore we selected a few patients randomly with 30 minutes length from MIT-BIH benchmark with sampling frequency 360 Hz to extract and mix slow oscillatory modes to fabricate 26 the artificial baselines including 25,000 samples.

3.1. Evaluation

In order to quantitative assessment of the methods correlation between the added baselines and extracted one (R), signal-to-baseline ratio (SBR), and reconstructed-to-clean signal power ratio (RCPR) were considered:

$$P_r = 10 * log10(\sum_{t=1}^{T}(x_b(t) - \widetilde{bw}(t))^2 \quad (10)$$

$$RCPR = \frac{P_r - P_o}{P_o} \times 100 \quad (11)$$

$$SBR = \frac{\sum_{t=1}^{T}(x_b(t))^2}{\sum_{t=1}^{T}(x_b(t) - \tilde{x}(t))^2} \quad (12)$$

$$R = \frac{\sum_{t=1}^{T} bw(t).\widetilde{bw}(t)}{\left(\sum_{t=1}^{T} bw(t)^2 . \sum_{t=1}^{T} \widetilde{bw}(t)^2\right)^{1/2}} \quad (13)$$

where $\widetilde{bw}(t)$ and $\tilde{x}(t)$ show reconstructed baseline and signal, respectively, P_r is power of the reconstructed signal in dB, and P_o is the power of clean signal.

Table I shows the average values obtained from 26 subjects for each method. In each table, the correlation column represents the similarity between the added baseline and the obtained result from the baseline correction.

Tabel 1. Obtained results from global slope minimization (GSM), emd-based polynomial fitting (EPF), and moving average filtering (MAF). Correlation between the added baselines and the extracted one (R), the signal-to-baseline ratio (SBR), and the reconstructed-to-clean signal power ratio (RCPR).

Methods	R	RCPR	SBR=13.36
GSM	0.26	3.40	1.73
EPF	0.81	0.30	12.28
MAF	0.73	-0.34	7.28

In the second column of Tables 1, the RCPR values show the percentage of diminishment in the power of the reconstructed signal in respect to the clean signal. RCPR can have both negative and positive values. The minus value shows that the reconstructed signal has lower power than the clean ECG signal, while the positive value demonstrates that the reconstructed signal carries some amount of the artificial baseline's power undesirably. Therefore, acceptable performance for the baseline correction is reached when the RCPR's value is close to zero.

The third column in Tables 1 includes SBR values which compares the power of the corrupted signal in proportion to the power of the baseline. The ideal SBR value is given by substituting the clean ECG signal for $\tilde{x}(t)$ which was averagely 13.36 in this study. As you can see EPF shows the closest SBR to the ideal value of SBR.

Of all three methods, EPF has the highest correlation, lowest RCPR and closest SBR to the ideal value which shows the ability of EPF to extract baselines from ECG data. It is worth to mention that majority of dissimilarity in EPF and GSM results from boundary effect in EMD technique which can be reduced by ensemble EMD and doubly iterative EMD methods [15, 16].

Fig. 2 depicts MSE versus removing last IMFs. The changes are not strictly descending, however after removing specific number of lower oscillatory modes,

MSE becomes close to zero. Hence, putting a low threshold on this variable, the true number of contributing IMFs can be determined. For example, for ECG signal in Figure 1, after removing 9th IMF from reconstructed signal the baseline remarkably vanished.

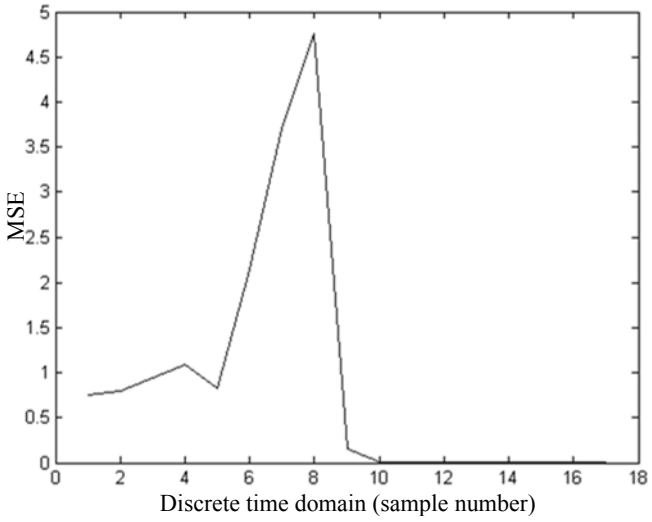

Figure 2. MSE changes in removing last IMFs for the ECG signal in Figure 1 using EMD-based polynomial fitting method.

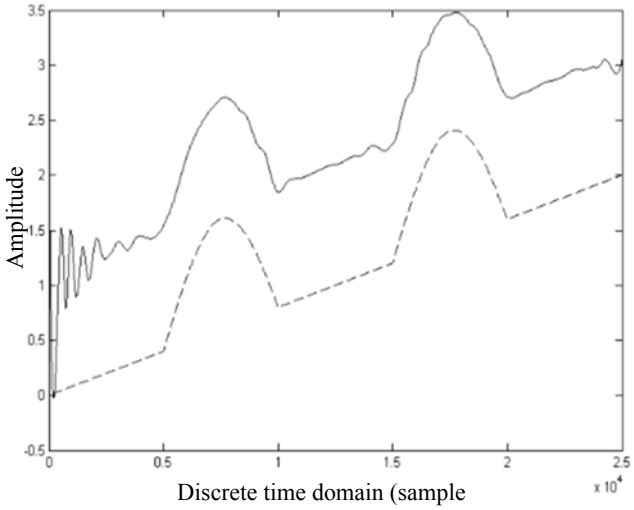

Figure 3. Extracted baseline from ECG signal in Figure 1. using EMD-based polynomial fitting method. The dashed line shows the added baseline and solid line denotes the extracted baseline.

The extracted baseline using polynomial baseline modeling is shown in Figure 3 where dashed line with border effects represents the estimated baseline using EMD approach. Comparing the artificial baseline in lower part of the figure with extracted baseline in higher part shows that EPF method has been successful, except that EMD method suffers from unwanted ripples on end sides. The reason for a constant distance between original baseline and extracted ones is that EMD methods accommodate the DC term of original signals in them.

References

[1] Hemmings HC Jr, Hopkins PM. Foundations of anesthesia: basic sciences for clinical practice, Elsevier Health Sciences, 2006.

[2] Blanco-Velasco M, Weng B, Barner KE. ECG signal denoising and baseline wander correction based on the empirical mode decomposition. Comput Biol Med 2008;38:1-13.

[3] Agrawal S, Gupta A. Fractal and EMD based removal of baseline wander and powerline interference from ECG signals. Comput Biol Med 2013;43:1889-1899.

[4] Kaur M, Singh B, Seema. Comparison of different approaches for removal of baseline wander from ECG signal. In Proc International Conference; Workshop on Emerging Trends in Technology 2011;1290-1294.

[5] Van Alste J, Schilder T. Removal of base-line wander and power-line interference from the ECG by an efficient FIR filter with a reduced number of taps. IEEE Transactions on Biomedical Engineering 1985;32:1052-1060.

[6] Laguna P, Jané R, Caminal P. Adaptive filtering of ECG baseline wander. In Engineering Medicine Biology Soc, 14th Annual International Conf IEEE 1992:508-509.

[7] Shusterman V, Shah SI, Beigel A, Anderson KP. Enhancing the precision of ECG baseline correction: selective filtering and removal of residual error. Computers and Biomedical Research 2000;33:144-160.

[8] Łęski JM, Henzel N. ECG baseline wander and powerline interference reduction using nonlinear filter bank. Signal Process 2005;85:781-793.

[9] Park K, Lee K, Yoon H. Application of a wavelet adaptive filter to minimise distortion of the ST-segment. Medical Biological Engineering Computing 1998;36:581-586.

[10] Von Borries R, Pierluissi J, Nazeran H. Wavelet transform-based ECG baseline drift removal for body surface potential mapping. In Engineering in Medicine and Biology Society, 27th Annual International Conference of the IEEE-EMBS 2005:3891-3894.

[11] Chawla M. PCA and ICA processing methods for removal of artifacts and noise in electrocardiograms: A survey and comparison. Applied Soft Computing 2011;11:2216-2226.

[12] Hyvärinen A, Oja E. Independent component analysis: algorithms and applications. Neural Networks 2000;13: 411-430.

[13] Echeverria J, Crowe J, Woolfson M, Hayes-Gill B. Application of empirical mode decomposition to heart rate variability analysis. Medical and Biological Engineering and Computing 2001;39:471-479.

[14] Hadj Slimane Z, Naït-Ali A. QRS complex detection using empirical mode decomposition. Digital Signal Processing 2010;20:1221-1228.

[15] Chang K. Arrhythmia ECG noise reduction by ensemble empirical mode decomposition. Sensors 2010;10:6063-6080.

[16] Kopsinis Y, McLaughlin S. Empirical mode decomposition based denoising techniques. 1st International Work-Shop on Cognitive Information Processing (CIP), 2008.